NANOSYSTEMS:
PHYSICS, CHEMISTRY, MATHEMATICS

Original article

Gatina E.N., Maslennikova T.P. *Nanosystems: Phys. Chem. Math.*, 2024, **15** (3), 380–387.
http://nanojournal.ifmo.ru
**DOI 10.17586/2220-8054-2024-15-3-380-387**

# Formation of chrysotile nanotubes with titania in the internal channel

Elmira N. Gatina, Tatiana P. Maslennikova

I. V. Grebenshchikov Institute of Silicate Chemistry, St. Petersburg, Russia

Corresponding author: Elmira N. Gatina, gatina.en@iscras.ru

ABSTRACT The paper studies the influence of titanium-containing compounds on the formation of hydrosilicate nanotubes under hydrothermal conditions. The possibility of titanium ions to enter the crystal structure, and of titania the nanotube channel, has been analyzed. The influence of temperature on the ratio of compounds forming under hydrothermal conditions was determined.

KEYWORDS nanoparticles, nanotubes, chrysotile, lizardite, morphology, hydrothermal synthesis, magnesium titanate, anatase, rutile

ACKNOWLEDGEMENTS TEM was performed by D. A. Kirilenko (the Ioffe Institute) using the equipment of the Joint Research Center 'Materials science and characterization in advanced technology' (Unique project identifier RFMEFI62117X0018). The present work was supported within the framework of the State Assignment No. 1023032900322-9-1.4.3

FOR CITATION Gatina E.N., Maslennikova T.P. Formation of chrysotile nanotubes with titania in the internal channel. *Nanosystems: Phys. Chem. Math.*, 2024, **15** (3), 380–387.

## 1. Introduction

Both halloysite and chrysotile hydrosilicate nanotubes can be promising for use as fillers of composite materials [1–8], as quasi-one-dimensional and nanotubular particles in modern devices, in technology and medicine [9–22], as well as precursors for the production of new materials [23–32]. Despite the existence of an extensive natural stock of nanotubular halloysite and chrysotile particles [33], their synthetic analogues have a number of advantages. This refers primarily to chrysotile nanotubes, since information on the synthesis of nanotubular halloysite is very limited. Apparently, the synthesis of the halloysite $Al_2Si_2O_5(OH)_4$ compound free from other ions impurities was described for the first time in [34]. The difficulties of synthesizing halloysite and the possibilities of overcoming them were analyzed in [35,36]. The publication of [34] was followed by a number of works [18, 37–39], in which halloysite nanotubular particles were also obtained. Theoretical aspects of the formation of crystalline nanotubular structures of any composition and structure were discussed in detail in [40–46]. Still, experimentally, the synthesis of only chrysotile nanotubes of different composition and morphology under different conditions and from different precursors has been studied in more detail [47–58]. Therefore, studies of the behavior and properties of nanotubes depending on their composition, morphological and dimensional parameters, use chrysotile hydrosilicate nanotubes, as a rule [59–61], the synthesis methods and conditions for which are widely presented in the literature [62, 63]. One of the advantages of synthetic materials, including nanotubes, compared to the use of natural raw materials, is the possibility of producing them with a strictly specified composition, morphology and particle size [64, 65]. Another important advantage of synthetic analogs over natural chrysotile that should also be noted is their significantly lower toxicity, which was shown in [66]. This advantage is especially important because the toxicity of chrysotile often limits its practical use [67–71].

Chrysotile structure is characterized by the possibility of isomorphic substitution of cations in both the octahedral and tetrahedral sublattices. This was noted in many works devoted to both natural minerals [72,73] and synthetically produced nanotubes [48–58, 65, 74]. At the same time, the high specific surface area, the large thickness of the interlayer gaps, the presence of channels which can also harbor impurity components [75–78], makes the answer to the question about the impurity localization ambiguous, i.e. it can be localized either in the crystal structure (in the octahedral/tetrahedral cation positions), inside the channels, in interlayers, or on the nanotube surface. Depending on their localization, impurity components can affect the structure and properties of nanoparticles in various ways.

Titania may be of significant interest as a modifying additive in the synthesis of chrysotile nanotubes. In [25, 79], the titania component was introduced onto the surface of nanotubes by the molecular layering method. In [75, 80, 81] devoted to the analysis of the natural chrysotile, it was proposed to consider $Ti^{4+}$ ions as isomorphically substituting $Mg^{2+}$ ions localized in the octahedral sublattice. At the same time, a possibility of entrance of a very small amount of titanium ions into the magnesium sublattice was pointed out.

In connection with the above reasons, it is relevant to study the nature of titania impurities localization during the formation of hydrosilicate nanotubes under hydrothermal conditions, including the introduction of titanium-containing additives in the form of various chemical compounds.

## 2. Experimental

Compounds obtained from the interaction of MgO and $TiO_2$ taken at 1:1 mole ratio were used as a titania additive for the introduction into the reaction system. The solid-phase synthesis of the additive was carried out by heat treatment of a mixture of $MgCO_3$ (p.a.) and $TiO_2$ (as Aldrich anatase). The initial components were mixed in a planetary mill, tablets were pressed and calcinated sequentially at 850, 1100 and 1250 °C.

Magnesium hydrosilicate was synthesized under hydrothermal conditions in aqueous solutions of NaOH with a 0.23 M concentration, isothermal exposure for 24 hours at 300 and 350 °C, and $\sim$ 70 MPa. The components were taken based on the chrysotile $Mg_3Si_2O_5(OH)_4$ stoichiometry ($MgO:SiO_2$ = 3:2). MgO (p.a.) and $SiO_2$ (large fine-porous granular silica gel, GOST 3956-76) were used as the starting components. Additionally, a pre-prepared titanium-containing additive (calculated as about 6 wt. % in terms of titania) was introduced into the reaction medium.

The shape and size of nanoparticles and the nanotube channel filling parameters were determined using the transmission electron microscopy (TEM) on a JEM 2100-F with an accelerating voltage Uac up to 200 kV. Dimensional parameters, morphology and elemental analysis of the samples were also determined by scanning electron microscopy (SEM) and EDX analysis performed on a Tescan Vega 3 SBH (Tescan, Czech Republic) with an EDX analysis attachment (Oxford Instruments, England).

The phase ratio, crystal structure parameters, and crystallite size of the samples were determined using the X-ray powder diffractometry data. These studies were carried out on a DRON-3M X-ray diffractometer (Bourevestnik Innovation Center, Russia) in the reflection mode (Bragg–Brentano geometry) using Cu$K\alpha$ radiation ($\lambda = 1.54$ Å, nickel $\beta$-filter). The obtained data were processed and peaks identified using the DFWin software package and the ICDD PDF-2 database, as well as the Rietveld method, and the software described in [82].

The specific surface area was determined from the low-temperature adsorption data (BET method). Measurements were made using a Nova 1200e instrument (Quantochrome).

## 3. Results and discussion

The X-ray diffraction pattern of a titanium-containing sample after heat treatment at 1250 °C shows that $MgTi_2O_5$, $MgTiO_3$, and MgO coexist in it as the main phases (Fig. 1). The ratio of the proportions of all the obtained compounds calculated by the Rietveld method and presented in Table 1, made it possible to determine the Mg:Ti mole ratio as 54:46, which, taking the error of X-ray analysis into account, is close to the (nominal) Mg:Ti ratio of 50:50 specified for the synthesis.

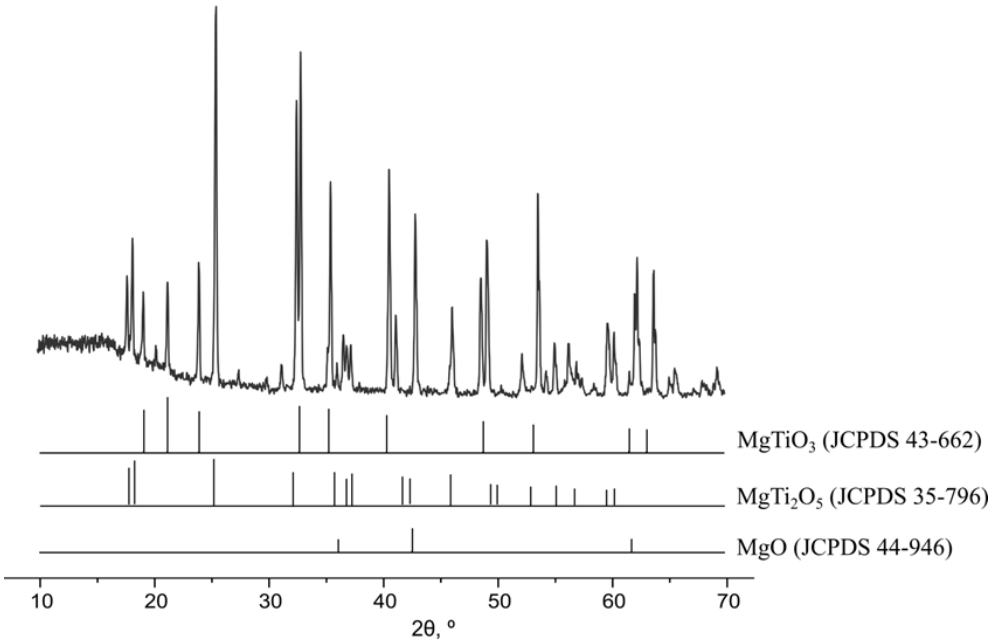


FIG. 1. X-ray diffraction pattern of a sample of the titana additive after heat treatment at 1250 °C. The data on the main compounds detected in the sample are presented as bar diagrams

The X-ray diffractometry data on samples after hydrothermal treatment indicate their multiphase nature; the main peaks are indicated in Fig. 2. The phase ratio calculated from these diffraction patterns shows that the introduction of even a small amount of titanium-containing additive ($\sim$ 6 wt.% in terms of titania) into the reaction system significantly affects the phase composition of the reaction products, which varies depending on the hydrothermal treatment temperature (Table 2).

TABLE 1. Phase composition of compounds after heat treatment at 1250 °C according to quantitative X-ray analysis carried out using the software package [82]

| Mg:Ti mole ratio (nominal ratio / calculation based on X-ray diffractometry data) | Phase composition according to X-ray diffractometry data, wt. % / mol. % | | | | |
|---|---|---|---|---|---|
| | $MgTiO_3$ | $TiO_2$ (rutile) | $MgTi_2O_5$ | $Mg_2TiO_4$ | MgO |
| 50:50 / 54:46 | 27.0 / 24.9 | 1.2/ 1.6 | 51.0 / 28.2 | 5.7 / 3.9 | 15.1 / 41.4 |

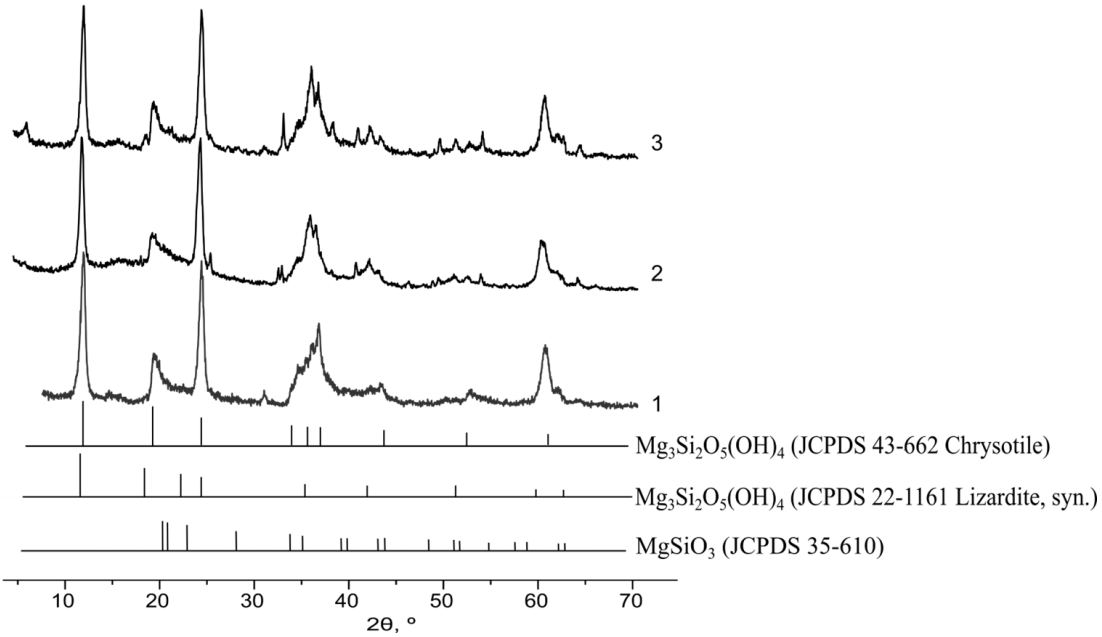


FIG. 2. X-ray diffraction patterns of samples Nos. 1, 2 and 3 (Table 2) after hydrothermal treatment. The data on the main compounds detected in the samples are presented as bar diagrams

TABLE 2. Phase composition of samples Nos. 1, 2 and 3 after hydrothermal treatment under different conditions ($T$, °C; $P \approx 70$ MPa), according to X-ray diffractometry data

| No. | $T$, °C | Mole ratio of compounds in reaction products, mol. % | | | | | | |
|---|---|---|---|---|---|---|---|---|
| | | $Mg_3Si_2O_5(OH)_4$ (chrysotile + lizardite) | $Mg_3Si_4O_{10}(OH)_4$ (vermiculite) | $MgSiO_3$ | $MgTiO_3$ | $MgTi_2O_5$ | $TiO_2$ (rutile) | $TiO_2$ (anatase) |
| 1 | 350 | 100 | — | — | — | — | — | — |
| 2 | 300 | 93.6 | — | 1.9 | 1.6 | 1.3 | 1.6 | — |
| 3 | 350 | 83.8 | 0.2 | 12.1 | 2.7 | — | 0.2 | 1.0 |

Note: sample No. 1 synthesized without addition of titania; samples Nos. 2 and 3 synthesized with the introduction of a titanium-containing oxide additive ($\sim$ 6 wt.% in terms of titania)

Comparison of the data given in the Table 3, based on the nominal elemental composition of the samples and determined by different methods, shows their agreement within the error limits of the methods. Therefore, these data allows us to assume that the elemental composition of the samples corresponds to the specified one.

TABLE 3. Mg:Si:Ti mole ratio

| Sample No. | Mg:Si:Ti mole ratio | | |
|---|---|---|---|
| | Nominal | Calculated from the X-ray diffractometry data | EDX |
| 1 | 58:42:(–) | 58:42:(–) | (63±2):(37±2):(–) |
| 2 | 57.2:38.9:3.9 | 59.5:39.3:1.2 | — |
| 3 | 57.2:38.9:3.9 | 58.7:39.7:1.5 | (63.7±1.7):(36.0±1.6):(0.3±0.1) |

The size of the rutile-structured titania crystallites calculated from the X-ray diffractometry data for the sample after hydrothermal treatment at 300 °C, was about 8 nm. The sample obtained by hydrothermal treatment at 350 °C had rutile crystallites of $\sim 160$ nm, and the anatase-structured titania crystallites were about 3 nm.

The differences in the parameter values of unit cells of the chrysotile nanotubes in samples Nos. 1, 2 and 3 do not exceed the error limits of the analytical method. This may be due to the extremely insignificant replacement of magnesium and silicon cations in nanoscrolls with $Ti^{4+}$ ions. This conclusion correlates with the data in [75, 80, 81], in which the entrance of extremely few titanium ions in the magnesium sublattice of natural chrysotile was noted. The slight replacement of magnesium ions with $Ti^{4+}$ ions [75, 80, 81] can be associated with both the difference in their ionic radii ($R_{\text{Mg2+(VI)}} = 0.86$ Å, $R_{\text{Ti4+(VI)}} = 0.745$ Å [83] and with the energy for charge compensation when $Mg^{2+}$ ions are replaced with $Ti^{4+}$. At the same time, the possibility of some replacement of $Si^{4+}$ with $Ti^{4+}$ ions in the tetrahedral (silicon) sublattice cannot be excluded, although a comparison of the ionic radii $R_{\text{Si4+(IV)}} = 0.40$ Å with $R_{\text{Ti4+(IV)}} = 0.56$ Å [83] shows their significant difference. The ionic radius of $Ge^{4+}$ ions is known to be close to that of $Ti^{4+}$ ions in the tetrahedral position ($R_{\text{Ge4+(IV)}} = 0.54$ Å, $R_{\text{Ti4+(IV)}} = 0.56$ Å [83]), and [36] demonstrated the possibility of $Si^{4+}$ cations replacement with $Ge^{4+}$ cations, and stabilization of the nanotubular structure of halloysite, structurally inverse with respect to the chrysotile structure. Both options for the replacement of both magnesium and silicon ions with titanium ions in magnesium hydrosilicate lead to the chrysotile structure destabilization due to a decrease in differences in the size of the octahedral and tetrahedral sublattices and, consequently, to a decrease in the energy effect from the transformation of a flat layer into a cylinder [40, 43]. Apparently, this is related to the fact that even a slight replacement of cations in the structure of magnesium hydrosilicate with $Ti^{4+}$ ions, which is poorly detected by changes in unit cell parameters, leads to a noticeable increase in the lamellar forms of magnesium hydrosilicate according to X-ray diffraction patterns (Fig. 2).

A comparison of the results on the nanoscrolls length distribution, obtained from the scanning electron microscopy data for samples with and without the introduced titanium-containing additive shows that the influence of the additive on the nanoscrolls dimensional parameters is small. A similar statement applies to the effect of the hydrothermal treatment temperature on the outer diameter distribution of nanoscrolls determined from the TEM data.

The TEM data (Fig. 3) show that the channel in a number of nanotubes is partially enriched in a substance containing elements that are heavier than magnesium and silicon. Since only titanium acts as such an element in this case, it is natural to conclude that it is the titanium-containing oxide that is located in the nanotube channel, and since the average crystallite sizes of only titania (rutile-structured after hydrothermal treatment at 300 °C, and anatase-structured after hydrothermal treatment at 350 °C) are comparable with the dimensions of the nanotube channel diameter (Fig. 3), then the nanotubes are filled with titania. During hydrothermal treatment at 300 °C, titania nanoparticles have a structure of rutile with an average crystallite size of about 8 nm. The particles in the channel have an elongated shape that repeats that of the channel with average dimensions of length $L_{\text{TiO2}} \approx 37 \pm 16$ nm and width $d_{\text{TiO2}} \approx 14 \pm 5$ nm. For empty nanotubes, the diameter of the internal space ($d_0$) is $\approx 12 \pm 3$ nm. An increase up to 350 °C leads to the localization of the main part of titana in the nanotube channel in the form of anatase with a crystallite size of about 3 nm, and a small part of titania (rutile-structured, with crystallites of about 160 nm) outside the channel. The distribution of nanotubes with the channel unfilled with titania according to their internal diameter is close to bimodal (Fig. 3). The average values of the internal diameter size distribution of these tubes are $d_{0(1)} \approx 17 \pm 3$ nm and $d_{0(2)} \approx 9 \pm 2$ nm. The distribution of nanotubes with a $TiO_2$-filled channel according to the size of their internal diameter has a clearly defined bimodal character (Fig. 3) with the internal diameter $d_{\text{TiO2(1)}} \approx 17 \pm 4$ nm and $d_{\text{TiO2(2)}} \approx 8 \pm 1$ nm. Anatase particles fill the channel in the form of discontinuous inclusions with a length $L_{\text{TiO2}} \approx 42 \pm 3$ nm and a width corresponding to the size of the nanotube inner diameter.

Titania-filled parts of nanotube channels alternate with the unfilled ones (see Fig. 3). Along with that, the characteristic lengths of the titana-filled parts of nanotube channels ($L_{\text{TiO2}}$) are comparable in length with the unfilled ones. It should

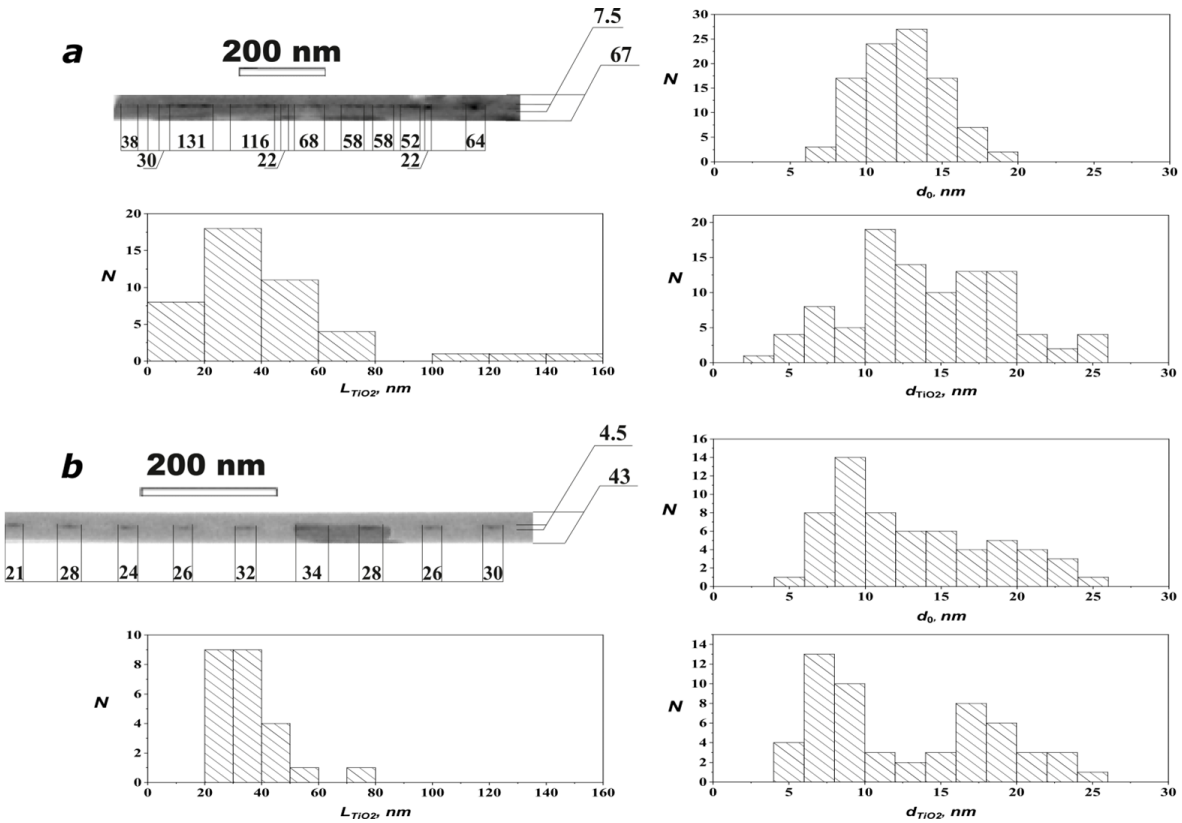


FIG. 3. TEM image of nanotubes with a titania additive obtained under hydrothermal conditions at: a) 300 °C and b) 350 °C, and the corresponding histograms of the length ($L_{\mathrm{TiO2}}$) distribution of nanotube titania-filled parts, as well as histograms of the internal diameter distribution of the unfilled ($d_0$), and of the titania-filled ($d_{\mathrm{TiO2}}$) nanotubes

be noted that the length ($L_{\mathrm{TiO2}}$) distribution of the titana-filled parts of nanotubes becomes narrower with the increasing temperature of hydrothermal treatment (Fig. 3). Taking into account the differences in the structural state (Table 2) and sizes of titania crystallites in cases of hydrothermal treatment at 300 and 350 °C, it can be concluded that almost all rutile-structured titania is localized inside the nanotube channel at 300 °C, while at 350 °C most of the titania in the form of anatase is located inside the channel, and a smaller part of the rutile-structured crystallites sized at about 160 nm is located outside the nanotube. Differences in the structural state of titania in nanotubes can apparently be associated with an increase in the proportion of nanotubes with a smaller channel diameter with the increase in temperature of hydrothermal treatment, since such changes in the size of spatial restrictions, as was shown in [84], lead to stabilization of the anatase structure of titania.

It is interesting to note that the parameters of intermittent filling ($L_{\mathrm{TiO2}}$ values) of the nanotube channels with titania correlate with the characteristic values of the size of chrysotile nanotube pre-nuclei [32, 85, 86] and with the values of the size of crystallites of which the nanotubes consist, as a rule [87]. This may testify in favor of the aggregation-accommodation mechanism [88] of nanoscrolls formation. It should be noted that the formation and stable existence of the above-described formations can be considered as a synthesis of core-shell type structures, in which the core is titania and the shell is a chrysotile nanotube [89, 90].

Some reduction in the specific surface area of samples obtained with the introduction of titanium-containing additives during the synthesis of hydrosilicate nanotubes under hydrothermal conditions from $S_{No.1} = 58.9$ m$^2$/g for sample No. 1 to $S_{No.2} = 42.4$ m$^2$/g and $S_{No.3} = 47.3$ m$^2$/g for samples Nos. 2 and 3, respectively, can be associated both with the formation of particles of the non-tubular structured compounds (Table 2) with small values of the specific surface area, and with the filling of channels of some part of nanotubes with titania, which prevents the entrance of gas into this channel. However, due to the small values these changes, they cannot be considered critical from the point of view of the use of materials based on such nanotubes in the cases when variations in the specific surface area are not of great importance for the effective functioning of the material.

## 4. Conclusions

It has been shown that when magnesium titanates are used as an additive in the hydrothermal synthesis of chrysotile, titania forms and localizes in channels of chrysotile nanotubes. At 300 °C of hydrothermal treatment, titania nanoparticles have a rutile structure with an average crystallite size of about 8 nm. The particles in the channel have an elongated shape, repeating that of the channel with average dimensions of length $L_{\mathrm{TiO2}} \approx 37 \pm 16$ nm and width $d_{\mathrm{TiO2}} \approx 14 \pm 5$ nm. An increase in the temperature of hydrothermal treatment up to 350 °C leads to the localization of the main part of titania in the nanotube channel in the form of anatase with the crystallite size of about 3 nm, and of a small part of titania outside the channel, with the rutile structure and the crystallite size of about 160 nm. Anatase particles fill the channel as discontinuous formations with sizes $L_{\mathrm{TiO2}} \approx 42 \pm 3$ nm, $d_{\mathrm{TiO2(1)}} \approx 17 \pm 4$ nm, and $d_{\mathrm{TiO2(2)}} \approx 8 \pm 1$ nm.

## References


[1] Gofman I.V., Svetlichnyi V.M., Yudin V.E., Dobrodumov A.V., Didenko A.L., Abalov I.V., Korytkova E.N., Egorov A.I., Gusarov V.V. Modification of films of heat-resistant polyimides by adding hydrosilicate and carbon nanoparticles of various geometries. *Russ. J. Gen. Chem.*, 2007, **77** (7), P. 1158–1163.

[2] Kononova S.V., Korytkova E.N., Romashkova K.A., Kuznetsov Y.P., Gofman I.V., Svetlichnyi V.M., Gusarov V.V. Nanocomposite based on polyamidoimide with hydrosilicate nanoparticles of varied morphology. *Russ. J. Appl. Chem.*, 2007, **80** (12), P. 2142–2148.

[3] Yudin V.E., Gladchenko S., Otaigbe J.U., Olson B.G., Nazarenko S., Korytkova E.N., Gusarov V.V. New polyimide nanocomposites based on silicate type nanotubes: Dispersion, processing and properties. *Polymer*, 2007, **48** (5), P. 1306–1315.

[4] Yudin V.E., Otaigbe J.U., Svetlichnyi V.M., Korytkova E.N., Almjasheva O.V., Gusarov V.V. Effects of nanofiller morphology and aspect ratio on the rheo-mechanical properties of polimide nanocomposites. *Express Polymer Letters*, 2008, **2** (7), P. 485–493.

[5] Kononova S.V., Korytkova E.N., Maslennikova T.P., Romashkova K.A., Kruchinina E.V., Potokin I.L., Gusarov V.V. Polymer-inorganic nanocomposites based on aromatic polyamidoimides effective in the processes of liquids separation. *Russ. J. Gen. Chem.*, 2010, **80** (6), P. 1136–1142.

[6] Yastrebinsky R.N. Nanodisperse hrizotilovy filler for heat-resistant radiation and protective composites. *Int. Research J.*, 2016, **8–3** (50), P. 123–129 (In Russian, abstract in English).

[7] Kononova S.V., Gubanova G.N., Korytkova E.N., Sapegin D.A. Polymer nanocomposite membranes. *Applied Sciences*, 2018, **8** (7), 1181.

[8] Kivilcim F.N. Development of halloysite loaded polypropylene sutures with enhanced mechanical and thermal properties. *Cumhuriyet Science J.*, 2023, **44** (1), P. 106–111.

[9] Yang Y., Liang Q., Li J., Zhuang Y., He Y., Bai B., Wang X. $Ni_3Si_2O_5(OH)_4$ multi-walled nanotubes with tunable magnetic properties and their application as anode materials for lithium batteries. *Nano Res.*, 2011, **4**, P. 882–890.

[10] Golubeva O.Y., Maslennikova T.P., Ulyanova N.Y., Dyakina M.P. Sorption of lead(II) ions and water vapors by synthetic hydro and aluminosilicates with layered, framework, and nanotube morphology. *Glass Phys. Chem.*, 2014, **40** (2), P. 250–255.

[11] Cheng L., Zhai L., Liao W., Huang X., Niu B., Yu Sh. An investigation on the behaviors of thorium(IV) adsorption onto chrysotile nanotubes. *J. Environ. Chem. Eng.*, 2014, **2** (3), P. 1236–1242.

[12] Yuan P., Tan D., Annabi-Bergaya F. Properties and applications of halloysite nanotubes: recent research advances and future prospects. *Appl. Clay Sci.*, 2015, **112–113**, P. 75–93.

[13] Bian Z., Li Z., Ashok J., Kawi S. A Highly active and stable Ni–Mg phyllosilicate nanotubular catalyst for ultrahigh temperature water-gas shift reaction. *Chem. Commun.*, 2015, **51**, P. 16324–16326.

[14] Chernyaev A.V., Mikhailin N.Y., Shamshur D.V., Kumzerov Y.A., Fokin A.V., Kalmykov A.E., Parfen'ev R.V., Sorokin L.M., Lashkul A. Electrical and magnetic properties of Pb and In nanofilaments in asbestos near the superconducting transition. *Physics of the Solid State*, 2018, **60** (10), P. 1935–1941.

[15] López-Salinas E., Toledo-Antonio J.A., Manríquez M.E., Sánchez-Cantú M., Cruz Ramos I., Hernández-Cortez J.G. Synthesis and catalytic activity of chrysotile-type magnesium silicate nanotubes using various silicate sources. *Micropor. Mesopor. Mater.*, 2019, **274**, P. 176–182.

[16] Krasilin A.A., Straumal E.A., Yurkova L.L., Khrapova E.K., Tomkovich M.V., Shunina I.G., Vasil'eva L.P., Lermontov S.A., Ivanov V.K. Sulfated halloysite nanoscrolls as superacid catalysts for oligomerization of hexene-1. *Russ. J. Appl. Chem.*, 2019, **92** (9), P. 1251–1257.

[17] Khrapova E.K., Ezhov I.S, Rumyantsev A.M., Zhdanov V.V., Krasilin A.A. Nanotubular nickel hydrosilicate and its thermal annealing products as anode materials for lithium ion batteries. *Inorg. Mater.*, 2020, **56** (12), P. 1248–1257.

[18] Golubeva O.Yu, Alikina Y.A., Kalashnikova T.A. Influence of hydrothermal synthesis conditions on the morphology and sorption properties of porous aluminosilicates with kaolinite and halloysite structures. *Appl. Clay Sci.*, 2020, **199**, 105879.

[19] Khrapova E.K., Ugolkov V.L., Straumal E.A., Lermontov S.A., Lebedev V.A., Kozlov D.A., Krasilin A.A. Thermal behavior of Mg-Ni-phyllosilicate nanoscrolls and performance of the resulting composites in hexene-1 and acetone hydrogenation. *Chem. Nano Mat.*, 2020, **7** (3), P. 257–269.

[20] Liu Z.Y., Zeng H., Wang L., Zhang Q., Wu P., Liu X., Xie H., Xiang W., Liu B., Liu J., Liu, X., Xie J., Tang J., Long Z., He L., Xiao M., Xiang L., Cao K. Fe-doped chrysotile nanotubes containing siRNAs to silence SPAG5 to treat bladder cancer. *J. Nanobiotechnol.*, 2021, **19** (1), 189.

[21] Yada M., Tabata M., Furukawa M. Synthesis and characterization of chrysotile/erythrosine composite to detect asbestos. *J. of the Ceramic Society of Japan*, 2023, **131** (12), P. 906–911.

[22] Long Q., Yan H., Zhou X., Qiu S., Qiu T. Adsorption and desorption characteristics of rare earth ions on halloysite surfaces. *Physicochem. Probl. Miner. Process*, 2024, **60** (1), 185763.

[23] Vezentsev A.I., Neiman S.M., Gudkova E.A. Transformations and changes in the properties of chrysotile asbestos under the influence of various factors. *Construction Materials*, 2006, **6**, P. 104–105 (In Russian).

[24] Malkov A.A., Korytkova E.N., Maslennikova T.P., Shtykhova A.M., Gusarov V.V. Effect of heat treatment on structural-chemical transformations in magnesium hydrosilicate $Mg_3Si_2O_5(OH)_4$ nanotubes. *Russ. J. Appl. Chem.*, 2009, **82** (12), P. 2079–2086.

[25] Kumzerov Yu.A., Naberezhnov A.A. Effect of restricted geometry on superconducting properties of low-melting metals (Review). *Low Temperature Physics*, 2016, **42** (11), P. 1028–1040.

[26] Gaaz T.S. Sulong A.B., Kadhum A.A.H., Nassir M.H., Al-Amiery A.A. Surface improvement of halloysite nanotubes. *Appl. Sci.*, 2017, **7** (3), 291.

[27] Krasilin A.A., Bodalyov I.S., Malkov A.A., Khrapova E.K., Maslennikova T.P., Malygin A.A. On an adsorption/photocatalytic performance of nanotubular $Mg_3Si_2O_5(OH)_4/TiO_2$ composite. *Nanosystems: Phys. Chem. Math.*, 2018, **9** (3), P. 410–416.

[28] Bloise A., Catalano M., Gualtieri A.F. Effect of grinding on chrysotile, amosite and crocidolite and implications for thermal treatment. *Minerals*, 2018, **8** (4), 135.

[29] Krasilin A.A., Danilovich D.P., Yudina E.B., Bruyere S., Ghanbaja J., Ivanov V.K. Crystal violet adsorption by oppositely twisted heat-treated halloysite and pecoraite nanoscrolls. *Appl. Clay Sci.*, 2019, **173**, P. 1–11.
[30] Belotitskii V.I., Fokin A.V., Kumzerov Y.A., Sysoeva A.A. Optical properties of nanowires synthesized in regular nanochannels of porous matrices. *Opt. Quant. Electron.*, 2020, **52** (4), 218.
[31] Krasilin A. Khalisov M., Khrapova E., Ugolkov V., Enyashin A., Ankudinov A. Thermal treatment impact on the mechanical properties of $Mg_3Si_2O_5(OH)_4$ Nanoscrolls. *Materials*, 2022, **15** (24), 9023.
[32] Maslennikova T.P., Gatina E.N., Kotova M.E., Ugolkov V.L., Abiev R.Sh., Gusarov V.V. Formation of magnesium hydrosilicate nanoscrolls with the chrysotile structure from nanocrystalline magnesium hydroxide and their thermally stimulated transformation. *Inorg. Mater.*, 2022, **58** (11), P. 1152–1161.
[33] Krivovichev S.V. Nanotubes in Minerals and Mineral-Related Systems. *Minerals as Advanced Materials I*, ed. Krivovichev S., 2008, P. 179–191.
[34] Maslennikova T.P., Korytkova E.N., Pivovarova L.N. Hydrothermal synthesis of nanotube composition $Al_2Si_2O_5(OH)_4 \cdot 2H_2O$ with halloysite structure. *Glass Phys. Chem.*, 2012, **S6**, P. 890–893.
[35] Krasilin A.A., Gusarov V.V. Control over morphology of magnesium-aluminum hydrosilicate nanoscrolls. *Russ. J. Appl. Chem.*, 2015, **88** (12), P. 1928–1935.
[36] Krasilin A.A. Energy modeling of competition between tubular and platy morphologies of chrysotile and halloysite layers. *Clays and Clay Minerals*, 2020, **68** (5), P. 436–445.
[37] White R.D., Bavykin D.V., Walsh F.C. Spontaneous scrolling of kaolinite nanosheets into halloysite nanotubes in an aqueous suspension in the presence of $GeO_2$. *J. Phys. Chem. C*, 2012, **116**, P. 8824–8833.
[38] Golubeva O.Y. Effect of synthesis conditions on hydrothermal crystallization, textural characteristics and morphology of aluminium-magnesium montmorillonite. *Micropor. Mesopor. Mater.*, 2016, **224**, P. 271–276.
[39] Leonov N.A., Kozlov D.A., Kirilenko D.A., Bert N.A., Pelageikina A.O., Nechitailov A.A., Alikin M.B., Krasilin A.A. Formation of a 10 Å phase with halloysite structure under hydrothermal conditions with varying initial chemical composition. *Nanosystems: Phys. Chem. Math.*, 2023, **14** (2), P. 264–271.
[40] Chivilikhin S.A., Popov I.Y., Gusarov V.V. Dynamics of nanotube twisting in a viscous fluid. *Doklady Physics*, 2007, **52** (1), P. 60–62.
[41] Chivilikhin S.A., Popov I.Y., Svitenkov A.I., Chivilikhin D.S., Gusarov V.V. Formation and evolution of nanoscroll ensembles based on layered-structure compounds. *Doklady Physics*, 2009, **54** (11), P. 491–493.
[42] Chivilikhin S.A., Popov I.Y., Bogdanov M.S., Lesnichii V.V., Gusarov V.V. Hydrodynamics of nanorolling. *Russ. Phys. J.*, 2009, **52** (11), P. 1117–1120.
[43] Krasilin A.A., Gusarov V.V. Energy of formation of chrysotile nanotubes. *Russ. J. Gen. Chem.*, 2014, **84** (12), P. 2359–2363.
[44] Krasilin A.A., Gusarov V.V. Energy model of bilayer nanoplate scrolling: Formation of chrysotile nanoscroll. *Russ. J. Gen. Chem.*, 2015, **85** (10), P. 2238–2241.
[45] Krasilin A.A., Gusarov V.V. Energy model of radial growth of a nanotubular crystal. *Technical Physics Letters*, 2016, **42** (1), P. 55–58.
[46] Krasilin A.A., Nevedomsky V.N., Gusarov V.V. Comparative energy modeling of multi-walled $Mg_3Si_2O_5(OH)_4$ and $Ni_3Si_2O_5(OH)_4$ nanoscrolls growth. *J. Phys. Chem. C*, 2017, **121** (22), P. 12495–12502.
[47] Korytkova E.N., Pivovarova L.N. Hydrothermal synthesis of nanotubes based on $(Mg,Fe,Co,Ni)_3Si_2O_5(OH)_4$ hydrosilicates. *Glass Phys. Chem.*, 2010, **36** (1), P. 53–60.
[48] Korytkova E.N., Maslov A.V., Pivovarova L.N., Drozdova I.A., Gusarov V.V. Formation of $Mg_3Si_2O_5(OH)_4$ nanotubes under hydrothermal conditions. *Glass Phys. Chem.*, 2004, **30** (1), P. 51–55.
[49] Korytkova E.N., Maslov A.V., Pivovarova L.N., Polegotchenkova Y.V., Povinich V.F., Gusarov V.V. Synthesis of nanotubular $Mg_3Si_2O_5(OH)_4$–$Ni_3Si_2O_5(OH)_4$ silicates at elevated temperatures and pressures. *Inorg. Mater.*, 2005, **41** (7), P. 743–749.
[50] Korytkova E.N., Pivovarova L.N., Semenova O.E., Drozdova I.A., Povinich V.F., Gusarov V.V. Hydrothermal synthesis of nanotubular Mg-Fe hydrosilicate. *Russ. J. Inorg. Chem.*, 2007, **52** (3), P. 338–344.
[51] Korytkova E.N., Pivovarova L.N., Drosdova I.A., Gusarov V.V. Hydrothermal synthesis of nanotubular Co-Mg hydrosilicates with the chrysotile structure. *Russ. J. Gen. Chem.*, 2007, **77** (10), P. 1669–1676.
[52] Korytkova E.N., Semyashkina M.P., Maslennikova T.P., Pivovarova L.N., Al'myashev V.I., Ugolkov V.L. Synthesis and growth of nanotubes $Mg_3Si_2O_5(OH,F)_4$ composition under hydrothermal conditions. *Glass Phys. Chem.*, 2013, **39** (3), P. 294–300.
[53] Krasilin A.A., Suprun A.M., Gusarov V.V. Influence of component ratio in the compound $(Mg,Fe)_3Si_2O_5(OH)_4$ on the formation of nanotubular and plate like particles. *Russ. J. Appl. Chem.*, 2013, **86**, P. 1633–1637.
[54] Krasilin A.A., Suprun A.M., Nevedomsky V.N., Gusarov V.V. Formation of conical $(Mg,Ni)_3Si_2O_5(OH)_4$ nanoscrolls. *Dokl. Phys. Chem.*, 2015, **460** (2), P. 42–44.
[55] Krasilin A.A., Panchuk V.V., Semenov V.G., Gusarov V.V. Formation of variable-composition iron(III) hydrosilicates with the chrysotile structure. *Russ. J. Gen. Chem.*, 2016, **86** (12), P. 2581–2588.
[56] Krasilin A.A., Suprun A.M., Ubyivovk E.V., Gusarov V.V. Morphology vs. chemical composition of single Ni-doped hydrosilicate nanoscroll. *Materials Letters*, 2016, **171**, P. 68–71.
[57] Krasilin A.A., Gusarov V.V. Redistribution of Mg and Ni cations in crystal lattice of conical nanotube with chrysotile structure. *Nanosystems: Phys. Chem. Math.*, 2017, **8** (5), P. 620–627.
[58] Krasilin A.A., Khrapova E.K., Nomine A., Ghanbaja J., Belmonte T., Gusarov V.V. Cations redistribution along the spiral of Ni-doped phyllosilicate nanoscrolls: energy modelling and STEM/EDS study. *Chem. Phys. Chem.*, 2019, **20** (5), P. 719–726.
[59] Kumzerov Y.A. Parfenyeva L.S., Smirnov I.A., Krivchikov A.I., Zvyagina G.A., Fil V.D., Misiorek H., Mukha Y., Ezhovsky A. Thermal and acoustic properties of chrysotile asbestos. *Phys. Solid State*, 2005, **47** (2), 370.
[60] Malkov A.A., Korytkova E.N., Maslennikova T.P., Shtykhova A.M., Gusarov V.V. Effect of heat treatment on structural-chemical transformations in magnesium hydrosilicate $[Mg_3Si_2O_5(OH)_4]$ nanotubes. *Russ. J. Appl. Chem.*, 2009, **82** (12), P. 2079–2086.
[61] Khrapova E.K., Ugolkov V.L., Straumal E. A., Lermontov S.A., Lebedev V.A., Kozlov D.A., Kunkel T.S., Nomine A., Bruyere S., Ghanbaja J., Belmonte T., Krasilin A.A. Front Cover: Thermal behavior of Mg-Ni-phyllosilicate nanoscrolls and performance of the resulting composites in hexene-1 and acetone hydrogenation. *Chem. Nano Mat.*, 2021, **7** (3), P. 257–269.
[62] Korytkova E.N., Pivovarova L.N., Gusarov V.V. Influence of iron on the kinetics of formation of chrysotile nanotubes of composition $(Mg,Fe)_3Si_2O_5(OH)_4$ under hydrothermal conditions. *Geochemistry Int.*, 2007, **45** (8), P. 825–831.
[63] Lafay R., Montes-Hernandez G., Janots E., Chiriac R., Findling N., Toche F. Nucleation and growth of chrysotile nanotubes in $H_2SiO_3/MgCl_2$/NaOH medium at 90 to 300 °C. *Chem. Eur. J.*, 2013, **19** (17), P. 5417–5424.
[64] Anuradha G., Esha B.S. A Descriptive review on nanosponges in novel drug delivery, synthetic methods, advantages and applications. *Int. J. of Pharmaceutical Sciences and Nanotechnology*, 2023, **16** (4), P. 6932–6941.

[65] Krasilin A.A., Khrapova E.K., Maslennikova T.P. Review: Cation doping approach for nanotubular hydrosilicates curvature control and related applications. *Crystals*, 2020, **10** (8), P. 654–695.
[66] Skuland T., Maslennikova T., Låg M., Gatina E., Serebryakova M.K., Trulioff A.S., Kudryavtsev I.V., Klebnikova N., Kruchinina I., Schwarze P.E., Refsnes M. Synthetic hydrosilicate nanotubes induce low pro-inflammatory and cytotoxic responses compared to natural chrysotile in lung cell cultures. *Basic Clin Pharmacol Toxicol.*, 2020, **126** (4), P. 374–388.
[67] Vezentsev A.I., Smolikov A.A., Pylev L.N., Vasilyeva L.A. Preparation of chrysotile asbestos and its isomorphic analogues and assessment of their carcinogenic activity. *J. of Environmental Chemistry*, 1993, **2**, P. 127–113 (In Russian).
[68] Bernstein D.M., Hoskins J.A. The health effects of chrysotile: current perspective based upon recent data. *Regul. Toxicol. Pharm.*, 2006, **45** (3), P. 252–264.
[69] Pylev L.N., Smirnova O.V., Vasil'eva L.A., Vezentsev A.I., Gudkova E.A., Naumova L.N., Neĭman S.M. Impact of modification of the fiber surface of chrysotile on its biological activity. *Gig Sanit*, 2007, **2**, P. 77–80 (In Russian).
[70] Gazzano E., Turci F., Foresti E., Putzu M. G., Aldieri E., Silvagno F., Lesci I.G., Tomatis M., Riganti C., Romano C., Fubini B., Roveri N., Ghigo D. Iron-loaded synthetic chrysotile: a new model solid for studying the role of iron in asbestos toxicity. *Chem. Res. Toxicol.*, 2007, **20** (3), P. 380–387.
[71] Vezentsev A.I., Pylev L.N., Poutlyayev V.I., Knot'ko A.V., Naumova L.N., Goudkova E.A., Smirnova O.V. Increase the ecological safety of chrysotile-asbestos due to action of Portland cement hydration. *Ecology and Industry of Russia*, 2009, **7**, P. 34–37 (In Russian).
[72] Liu X., Ma Y., Yan W., He M., Li L., Sui X., Peng B. Identify key serpentines antigorite, lizardite and chrysotile with various compositions and crystallographic orientations using micro-Raman spectroscopy. *Solid Earth Sciences*, 2023, **8** (4).
[73] Ono Y., Kikuchi N., Watanabe H. Preparation of nickel catalyst from nickel containing chrysotile. *Studies in Surface Science and Catalysis*, 1987, **31**, P. 519–529.
[74] Bloise A. Growth and Hydrothermal alteration of silicates doped with $Ti^{4+}$, $Ni^{2+}$: synthesis of Ni-, Ti-, Fe-serpentine phases. *Plinies*, 2006, **32**, P. 70–75.
[75] Maslennikova T.P., Korytkova E.N., Gusarov V.V. Interaction of $Mg_3Si_2O_5(OH)_4$ nanotubes with potassium hydroxide. *Russ. J. Appl. Chem.*, 2008, **81** (3), P. 375–379.
[76] Bloise A., Barrese E., Apollaro C. Hydrothermal alteration of Ti-doped forsterite to chrysotile and characterization of the resulting chrysotile fibers. *Neues Jahrbuch für Mineralogie – Abhandlungen*, 2009, **185** (3), P. 972–304.
[77] Maslennikova T.P., Korytkova E.N. Aqueous solutions of cesium salts and cesium hydroxide in hydrosilicate nanotubes of the $Mg_3Si_2O_5(OH)_4$ composition. *Glass Phys. Chem.*, 2010, **36** (3), P. 345–350.
[78] Maslennikova T.P., Gatina E.N. Modification of $Mg_3Si_2O_5(OH)_4$ nanotubes by magnetite nanoparticles. *Glass Phys. Chem.*, 2016, **43** (3), P. 257–262.
[79] Bodalyov I.S., Malkov A.A., Korytkova E.N., Maslennikova T.P., Malygin A.A. Temperature factor in interaction of nanotubular magnesium hydrosilicate, $Mg_3Si_2O_5(OH)_4$, with titanium tetrachloride and water vapors. *Russ. J. Appl. Chem.*, 2014, **87** (2), P. 151–159.
[80] Maslennikova T.P., Korytkova E.N., Gatina E.N., Pivovarova L.N. Effect of temperature on the synthesis of nanoparticles with different morphology in the system $MgO–SiO_2–TiO_2–H_2O$ under hydrothermal conditions. *Glass Phys. Chem.*, 2016, **42** (6), P. 627–630.
[81] Maslennikova T.P., Gatina E.N. Hydrothermal synthesis of Ti-doped nickel hydrosilicates of various morphologies. *Russ. J. Appl. Chem.*, 2018, **91** (2), P. 286–291.
[82] Bubnova R.S., Firsova V.A., Volkov S.N., Filatov S.K. RietveldToTensor: program for processing powder X-Ray diffraction data under variable conditions. *Glass Phys. Chem.*, 2018, **44** (1), P. 33–40.
[83] Shannon R.D. Revised effective ionic radii and systematic studies of interatomic distances in halides and chalcogenides. *Acta Crystallographica Section A*, 1976, **32**, P. 751–767.
[84] Almjasheva O.V. Formation and structural transformations of nanoparticles in the $TiO_2–H_2O$ system. *Nanosystems: Phys. Chem. Math.*, 2016, **7** (6), P. 1031–1049.
[85] Sharikov F. Y., Korytkova E. N., Gusarov V.V. Effect of the thermal prehistory of components on the hydration and crystallization of $Mg_3Si_2O_5(OH)_4$ nanotubes under hydrothermal conditions. *Glass Phys. Chem.*, 2007, **33** (5), P. 515–520.
[86] Krasilin A.A., Almjasheva O.V., Gusarov V.V. Effect of the structure of precursors on the formation of nanotubular magnesium hydrosilicate. *Inorg. Mater.*, 2011, **47** (10), P. 1111–1115.
[87] Levin A., Khrapova E., Kozlov D., Krasilin A., Gusarov V. Structure refinement, microstrains and crystallite sizes of Mg-Ni-phyllosilicate nanoscroll powders. *J. Appl. Cryst.*, 2022, **55** (3), P. 484–502.
[88] Almjasheva O.V., Gusarov V.V. Metastable clusters and aggregative nucleation mechanism. *Nanosystems: Phys. Chem. Math.*, 2014, **5**(3), P. 405–416.
[89] Almjasheva O.V., Krasilin A.A., Gusarov V.V. Formation mechanism of core-shell nanocrystals obtained via dehydration of coprecipitated hydroxides at hydrothermal conditions. N*anosystems: Phys. Chem. Math.*, 2018, **9** (4), P. 568–572.
[90] Almjasheva O.V., Popkov V.I., Proskurina O.V., Gusarov V.V. Phase formation under conditions of self-organization of particle growth restrictions in the reaction system. *Nanosystems: Phys., Chem. Math.*, 2022, **13** (2), P. 164–180.

*Submitted 22 November 2023; revised 25 December 2023; accepted 26 December 2023*

*Information about the authors:*

*Elmira N. Gatina* – I. V. Grebenshchikov Institute of Silicate Chemistry of the Russian Academy of Sciences, 2 Makarova Emb., 199034, St. Petersburg, Russia; ORCID 0000-0001-9294-4428; gatina.en@iscras.ru

*Tatiana P. Maslennikova* – I. V. Grebenshchikov Institute of Silicate Chemistry of the Russian Academy of Sciences, 2 Makarova Emb., 199034, St. Petersburg, Russia; ORCID 0000-0002-0872-7592; maslennikova.tp@iscras.ru

*Conflict of interest*: the authors declare no conflict of interest.